ATLAS Internal Note
INDET-NO-***
16 March, 1999

ATL-INDET-99-002
20/03/99

Comments on the Forward SCT Layout

Allan G. Clark, DPNC, University of Geneva

Tim Jones, Dept. of Physics, University of Liverpool

Alan Poppleton, CERN

Abstract

The Forward SCT layout was recently subject to discussion in the SCT community, and a new Forward Layout [1] was approved by the ATLAS SCT Institute Board on November 8, 1998. Several layouts are proposed which save one inner ring of silicon detectors, without significant degradation of the detector performance.

Following an initial presentation of the contents of this note, we were requested by the SCT community to provide a final detector design for all rings of the Forward detector. This has been done, and is shown to give a (marginally) improved performance.

1 Introduction and Summary.

The TDR Forward SCT layout [2] was recently replaced as the baseline by a new layout [1], approved by the SCT Institute Board on November 8, 1998. This new baseline layout (NB), which was optimized by requirements of track hermeticity and recommended by the SCT Steering Group, was motivated by

- a slightly increased inner active radius for the forward disks, required by the pixel forward disk locations,
- a total (outer module to outer module) disk thickness of 34mm, stated to be the minimum guaranteed for engineering reasons (cooling pipe and block routing),
- a slightly increased effective radius for each SCT barrel, to take account of the 10^o module tilt at the barrel - forward interface, and tiling effects.

A consequence of the new layout was a re-design of the inner and middle detector dimensions (the W11, W21 and W22 detectors), and the addition of one complete inner module ring on wheel #2. For a marginal deterioration of detector hermeticity, which is small compared with the effect of bonding gaps, the additional inner module ring can be avoided, with consequent cost and material advantages. The pattern recognition properties of a new suggested layout are also slightly improved, because of a more regular wheel spacing.

In Section 2, we describe the new base-line (NB) layout, and we show the location of both gaps and overlaps within individual wheels of the layout. We show that the overlapping space-points created by tracks traversing modules of an individual wheel are significant, suggesting that a more optimised wheel and wafer design may be desirable. Because bonding gaps were not considered during optimization (which was on the basis of hermeticity) the NB layout introduced an additional inner ring.

In Section 3 we compare the NB layout with an alternative layout that uses the same detector, module and wheel geometry as for the NB layout, but does not include the additional inner ring. We conclude that, although there is a slight deterioration of performance, the benefit of an additional inner ring cannot be justified.

In Section 4, we return to the TDR layout. Assuming a disk thickness of 31 mm, we have retained the TDR detector designs, and have slightly shifted the module positions on each disk to maintain a radial overlap. We show the space point distribution of hits on the wheels, and we present a layout (called NEW-B) using the original detectors that fulfils the SCT tracker specifications.

The detector design of Section 4 is viable, and could be justified for slightly larger disk thicknesses. The layout was presented to the SCT IB in March 1999. It was noted that none of the above designs were optimal, and in particular that module overlaps significantly exceeded the design specifications of 1%. The SCT IB instructed the authors to return with revised active detector dimensions for *all* forward modules. Two new wheel designs - designated NEW-C and NEW-D - are described in Section 5. In the NEW-C design, all detectors are re-optimised, and in the design NEW-D, detectors of the inner and middle rings are re-optimised. The difference in performance is marginal. Each of the layouts NEW-B, NEW-C or NEW-D are feasible, and the SCT SG has been presented with the results in order to make an informed decision based on a performance - schedule - financial trade-off.

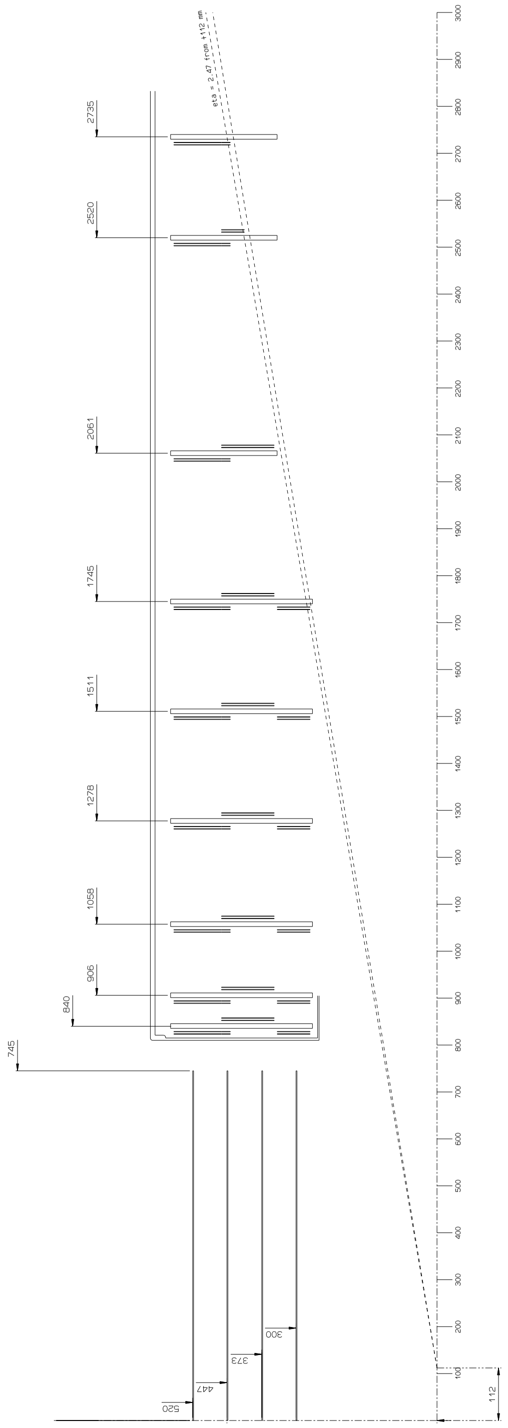

Figure 0-1 The New Baseline Layout for the Forward SCT Tracker (NB).

2 New Baseline (NB)Layout and Wheel Geometry.

Figure 0-1 shows the New Baseline (NB) layout, as approved by the SCT Institute Board. Table 1 shows the z-positions of each wheel, and compares the wheel positions to those of the TDR layout . Table 2 shows the radial position of each detector type on the wheel in the NB layout, and

Disk #	NB Layout (metres)	TDR layout (metres)
1	0.840	0.835
2	0.906	0.925
3	1.0575	1.072
4	1.2775	1.260
5	1.511	1.460
6	1.745	1.695
7	2.061	2.135
8	2.520	2.528
9	2.735	2.778

TABLE 1. Z-position of disks in the NB and TDR Layouts

the active detector dimensions.

Detector	W11	W21	W22	W31	W32
R_{min} (cm)	26.7634 (25.9190)	34.2666 (33.4916)	40.6554 (39.9825)	43.8765 (43.8666)	50.4445
R_{max} (cm)	33.8770 (33.1100)	40.4454 (39.7625)	45.7500 (45.1800)	50.2345 (50.2245)	56.0
Length (cm)	7.1136 (7,1910)	6.1788 (6.2715)	5.0946 (5.1975)	6.3580	5.5555
1/2 width lower (cm)	2.150	2.760	3.263	2.721	3.128
1/2 width upper (cm)	2.720	3.250	3.670	3.120	3.473

TABLE 2. Active detector radial positions and dimensions for the NB layout, and in brackets for the TDR layout. The bond gap is assumed to be 2.1 mm for the NB layout. An active angular strip coverage of 0.209 mrad has been assumed for the inner and middle rings, and 0.1615 mrad for the outer rings.

The layout differs from that of the TDR in the following respects:

- the addition of an inner module ring on disk #2, 'to improve the detector hermeticity',
- a disk thickness of 34 mm (outer module to outer module) which necessitates new detector designs for the inner and middle module rings (the TDR layout assumed a 26 mm gap)

- a bonding gap of 2.1mm, compared with the TDR design of 2.2 mm,
- a very short separation between the disks #1 and #2, which is undesirable,
- a reduced $|\eta|$ coverage, partly resulting from the constraints of a revised TRT envelope (including the disk #9 position)

In order to assess the hermeticity of individual full disks in the NB layout, a total of 10^7 straight tracks were generated uniformly in the range $1.0 < |\eta| < 2.5$. A Gaussian vertex spread with $\sigma = 5.6$ cm was assumed. The exact (active) detector geometry and position was described by the program. The barrel radius was assumed to that of the most outer silicon modules (the most pessimistic case). Hits were generated in detector elements traversed by each track, and space points were formed using the radial and stereo layers if

- back-to-back stereo detectors recorded hits enabling a space point evaluation within a given module,
- an R-Φ hit of one module, and a stereo hit of an adjacent module on the same side of the disk, allowed the creation of a space point (these are called 'Φ-overlap space points').

Figure 2 shows the distribution of space points reconstructed in a quadrant of wheel 6. The distribution of space points is uniform. Radial lines indicate some evidence for module overlaps, and a heavy band at R ~ 45 cm corresponds to the overlap of the central and outer modules. This band is artificially accentuated by the z-offset for which each space point is evaluated. A depletion of space points at R~40 cm and R ~ 51 cm correspond to *bond gaps* in the middle and outer modules respectively. The depletion of space points at R ~ 35 cm will be shown to be artificial, because of the z-offsets of the inner and middle modules. It is finally possible to evidence the trapezoid shape of the detectors, and the effect of the stereo detectors.

Figures 2-2 a) and 2-2 b) show the impact point of tracks for which no space point is reconstructed, in respectively wheels #1 and #6. While the dense inner and external bands ar e artificial from the known limits of wheel acceptance, band gaps for the middle and outer modules are pronounced. As in the case of barrel modules, Table 3 shows that typically 1.7% of all tracks within the wheel acceptance have no space point. Of this number only 0.05% (0.01%) of all space points lost are due to module gaps within respectively wheels #1 and #6. In pr evious optimization of the overlap on the basis of hermeticity, no account was taken of the bond gap, which is the *dominant* reason for the loss of space points within a wheel.

Figures 2-2 c) and 2-2 d), and Table 3 show the reconstructed space-point *overlaps* within a quadrant of the wheel, again for the extreme cases of Wheels #1 and #6 in the NB layout.

The specification which we assume is an overlap of 1% for alignment purposes, and hermeticity for prompt tracks of $p_T > 1$ GeV/c. In the least favourable case (wheel #1), the overlap r equired to maintain hermeticity at the outer radius of the outer (middle) rings is respectively 560 µm (374 µm). This corresponds to 6.2 (3.9) strips. The required overlap for hermeticity is reduced by a factor ~ 3 for wheel #9.

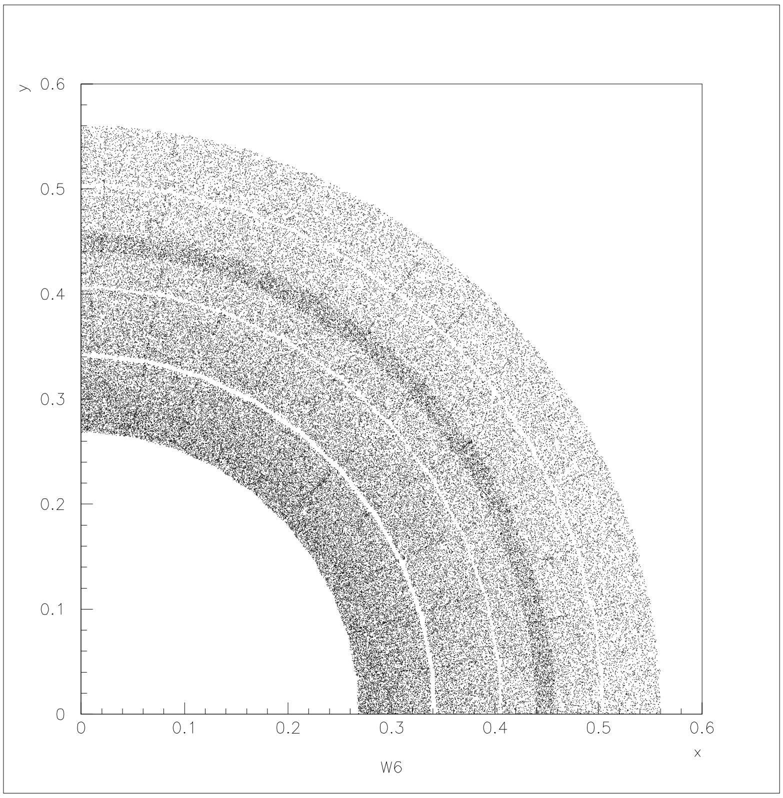

Figure 2-1 The distribution of reconstructed space points in a quadrant of wheel 6, for the NB layout.

,

	Wheel #1	**Wheel #6**
Gaps	$1.74\ 10^{-2}$	$1.70\ 10^{-2}$
Gaps (no Φ-overlap space points)	$1.88\ 10^{-2}$	$1.90\ 10^{-2}$
Overlaps in Φ	$2.19\ 10^{-2}$	$2.24\ 10^{-2}$
Overlaps in Φ (no Φ-overlap space points)	$0.75\ 10^{-2}$	$7.33\ 10^{-2}$
Overlaps in R(out)	$0.90\ 10^{-2}$	$3.41\ 10^{-2}$
Overlaps in R(out) (no Φ-overlap space point)	$0.88\ 10^{-2}$	$3.44\ 10^{-2}$
Overlap in R(in)	$3.13\ 10^{-3}$	$6.74\ 10^{-2}$
Overlap in R(in) (no Φ-overlap space point)	$3.09\ 10^{-2}$	$5.48\ 10^{-3}$

TABLE 3. Probability per track that no space point is reconstructed (gap), or that overlapping space points are reconstructed, for the NB layout in the range $1.0 < |\eta| < 2.47$.

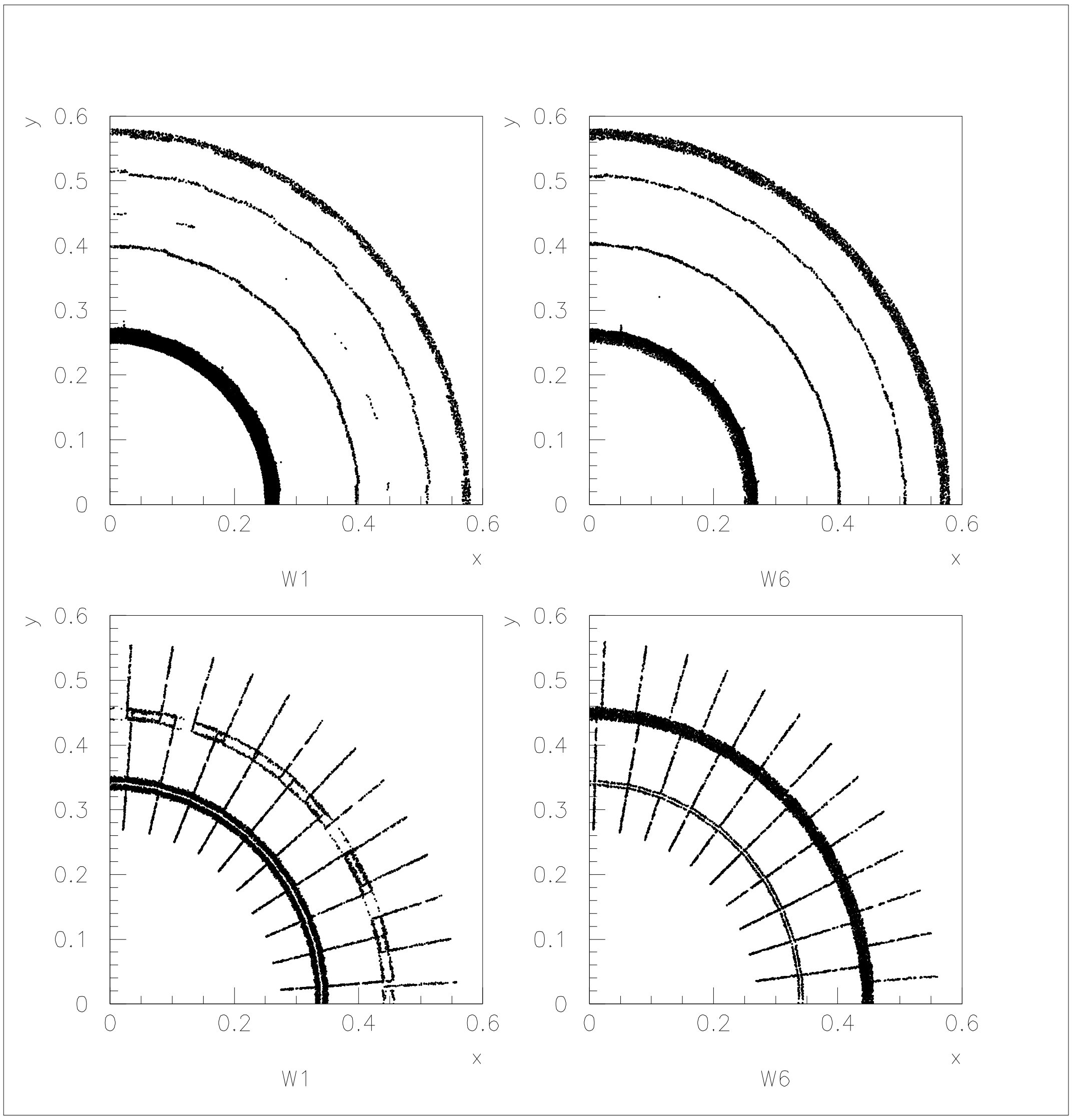

Figure 2-2 Tracks having no reconstructed space point in either wheels 1 (a) or 6 (b), for the NB layout. Figures c) and d) show, for the same wheels, events for which there are overlaps between modules [3].This plot includes the event category for which there are ‘Φ- overlap space points’.

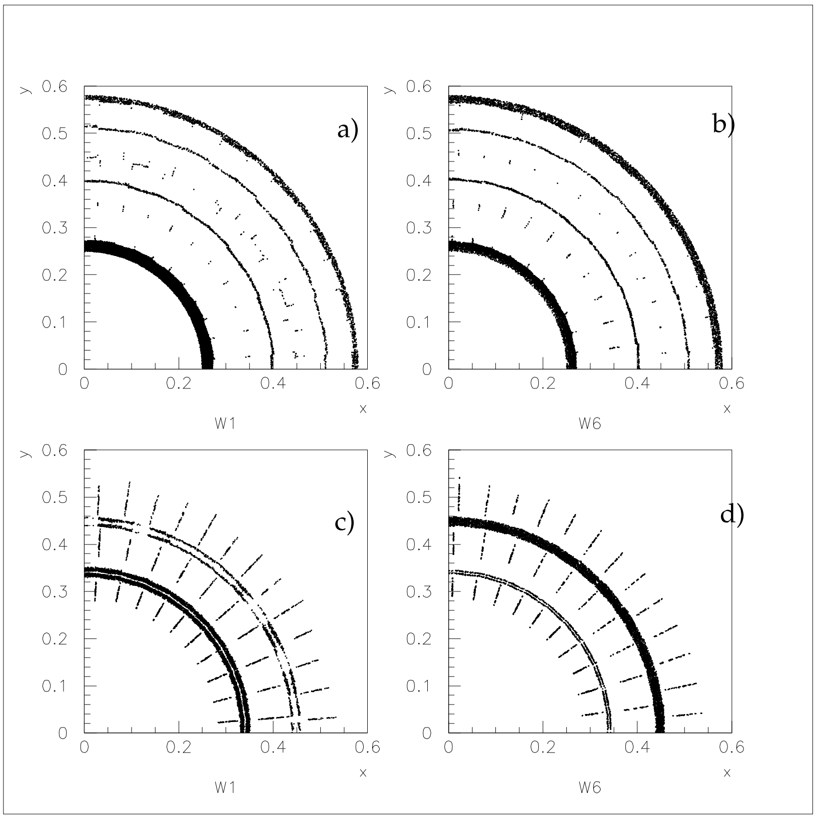

Figure 2-3 Tracks having no reconstructed space point in either wheels 1 (a) or 6 (b). Figures c) and d) show, for the same wheels, events for which there are overlaps between modules [3].This plot excludes the event category for which there are Φ- overlaps

The alignment requirement implies an overlap on each side of the detector of 1.24 mrad (0.62 mrad) for the outer ring and 1.605 mrad (0.805 mrad) for the middle ring, depending on whether the total overlap, or the overlap on each side, is assumed to be 1%. The actual overlap on each side for the NB layout is 1.601 mrad (outer ring) and 1.716 mrad (middle ring). A 0.5% overlap on each edge of the module is over-kill on the basis of rate.

	Wheel #1	**Wheel #6**
Gaps	$5.60\ 10^{-4}$	$1.13\ 10^{-4}$
Overlaps in Φ	$2.25\ 10^{-2}$	$2.30\ 10^{-2}$
Overlaps in R(out)	$8.97\ 10^{-3}$	$3.51\ 10^{-2}$
Overlaps in R(in)	$3.13\ 10^{-2}$	$5.63\ 10^{-3}$

TABLE 4. Probability per track that no space point is reconstructed (gap), or that overlapping space points are reconstructed, for the NB layout. Bond gaps are not included.

In Figures 2-3 a) through 2-3 d), and again in Table 3, the *same* plots are shown in the $|\eta|$ range $1.0 < |\eta| < 2.47$, when 'Φ-overlap space points' are not permitted. As can be seen some azimuthal gaps do result, at the level of ~ 10% of that due to bond gaps. For completeness, Table 4 shows, with the NB disk layout, the probability per track of gaps and overlaps if the bond gap is excluded.

In conclusion, the Φ–overlap of the NB detector designs has been overestimated, and should be reduced in any future detector design optimization. Gaps in Φ or radius are negligible compared with bond gaps. Further disk optimization is possible.

3 Optimization of the Layout using the NB Disk and Detector Geometry.

In this section we retain the disk and detector geometry of the NB layout, and we find a longitudinal geometry for individual wheels, that:

- provides good pattern recognition capability without the requirement of an inner module ring at disk #2,
- deteriorates minimally the detector hermeticity (in any case to a level that is much less than the loss due to bond gaps), and
- improves, with respect to the NB layout, the minimal radial separation between space points.

The layout has been constrained as follows:

- the z-positions of disks 1 and 9 are constrained to the NB positions, respectively because of the minimal barrel-forward separation (taking into account the increased disk thickness), and the revised TRT envelope,
- the inner ring of modules on wheel #2, introduced for the NB layout, has been removed,
- a constrained coverage of $|\eta| < 2.47$ (with respect to the unfavourable 2-σ vertex limit) is required,
- a disk thickness of 34 mm, and detector designs as in the NB layout are assumed, and
- a loss of hermeticity is attempted, which is reasonable distributed in $|\eta|$, and which does not exceed 10% for 4-point SCT tracks except at the barrel-forward interface (the 10% figure is qualitative, and chosen to correspond to the barrel hermeticity).

The geometry has been modelled including the exact trapezoid detector and stereo module designs and locations, including bond gaps. Straight tracks are generated randomly in azimuth and $|\eta|$, with a gaussian vertex spread of $\sigma = 56$ mm. Typically 10^7 tracks are generated in each configuration.

Following a qualitative re-optimization of the wheel positions, the z-positions as shown in Figure 3-1 and Table 5 are suggested. We call this layout NEW-A. We emphasise that the NEW-A layout can be further optimised.

Disk #	NEW-A Layout (metres)
1	0.84
2	0.930
3	1.09
4	1.263
5	1.457
6	1.670
7	2.070
8	2.445
9	2.735

TABLE 5. Z-position of disks in the NEW-A Layout.

Figure 3-2 a) compares the fractional loss of space points for the qualitatively optimised layout, and with the NB layout. Because of the additional inner ring on wheel #2, hermeticity is improved for the NB layout with an increased fraction of 5-point tracks. Table 6 compares the fractional rate of tracks with <4 reconstructed SCT space points, and < 3 reconstructed space points, for the NB and NEW-A layouts.

	NEW-A Layout	NB Layout
Fraction of tracks with <4 reconstructed SCT space points	0.070	0.056
Fraction of tracks with < 3 reconstructed SCT space points.	0.0023	0.00037

TABLE 6. Fraction of tracks with respectively < 4 and <3 reconstructed SCT space points, for the NEW-A and NB layouts, in the range $1.0 < |\eta| < 2.47$.

The important quantity for pattern recognition studies is the fraction of tracks with < 3 reconstructed SCT space points. The value of 2.3 per mil for the NEW-A layout results from the competing design requirement of maximising the wheel #1 - wheel #2 separation, and to pr ojective aligned bond gaps in the first 3 wheels. This was avoided in the NB layout at the expense of a closer wheel #1 - wheel #2 separation, with the intr oduction of an additional wheel to remove the consequent acceptance gaps at higher $|\eta|$. While the 2.3 per mil rate for the NEW-A layout can be further improved (see also Section 4), it is not believed possible to reach our design aim of ~ 1 per mil.

The loss of 4-point tracks in the NEW-A layout is similar to that in the barrel, and is dominated by bond gaps. The lower rate in the NB layout is partly artificial since 2 space points at low radius are close.

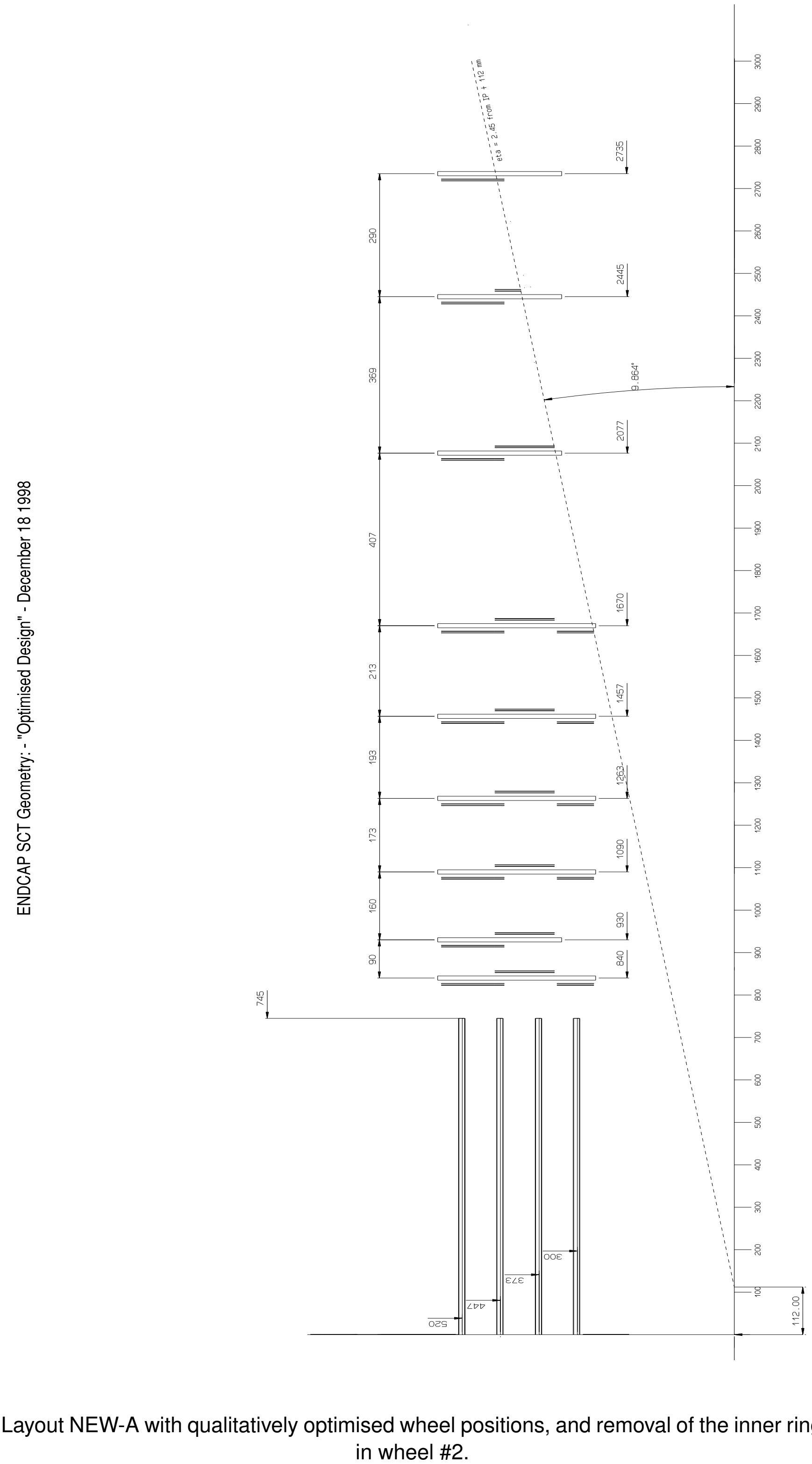

Figure 3-1 Layout NEW-A with qualitatively optimised wheel positions, and removal of the inner ring of modules in wheel #2.

The loss of hermeticity near the barrel-forward interface is in each case un-avoidable. As shown in Section 2, the NB layout has a large fractional overlap rate (with consequent material effects) in radius as well at azimuth. However, an adequate overlap is required for alignment purposes in the limiting cases at the outer radius of wheel #1 and the inner radius of wheel #6.

Figure 3-2 b) shows the minimum radial separation for 4-point tracks in each layout. Because of the decreased wheel #1 - wheel #2 separation, the radial separation between space points is small in the intermediate $|\eta|$ region for the NB layout. Although not ideal for either layout, the distribution of the NEW-A layout is more uniform.

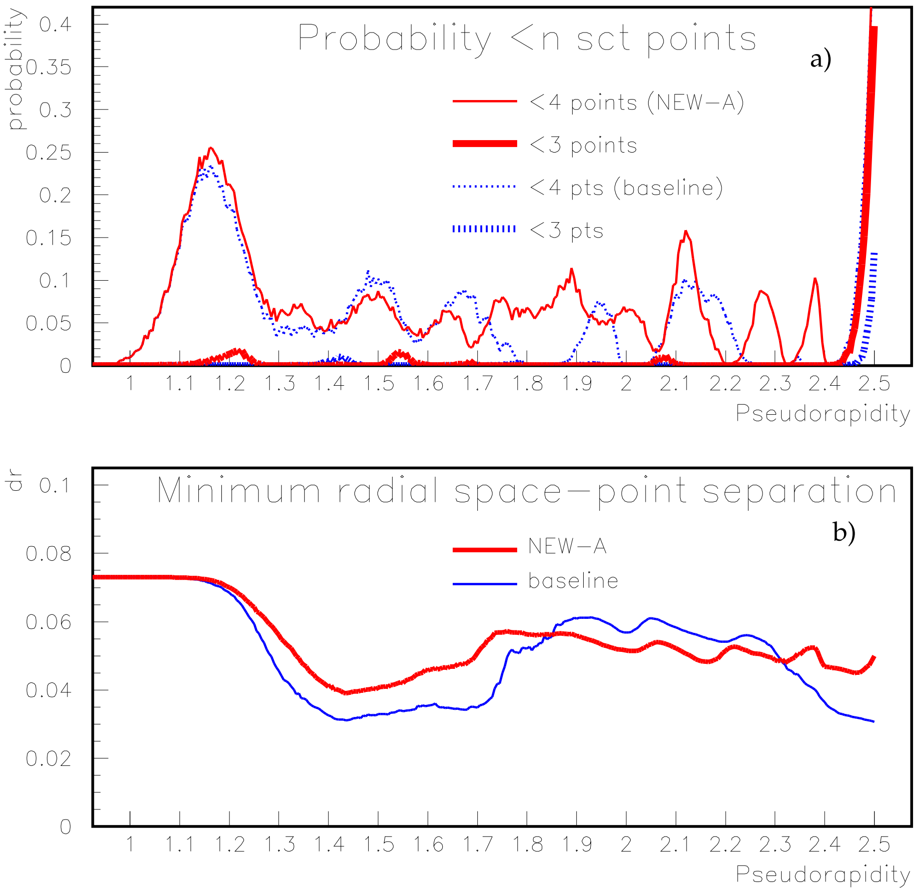

Figure 3-2 Fraction of tracks (a) as a function of $|\eta|$, for which respectively < 4 or <3 space points are reconstructed by the SCT. Both the NEW-A and NB layouts are shown. The figure (b) compares the minimum radial separation between reconstructed space points, for each layout.

4 A Realistic Layout (NEW-B) based on the TDR Detector Design.

Three implicit constraints of the NB and NEW-A layouts can now be revisited.

- The wheel thickness (outer module to outer module) was assumed for the purposes of detector optimization to be 34 mm, and with rather different optimization criteria. This can now, in the most pessimistic circumstances, be assumed to be 31 mm [3] (the result will be little changed for 32 mm).
- A requirement of the pixel envelope resulted in an increase of the minimum active radius for the forward SCT detectors. With the decision to relocate the pixel detectors, this is no longer a constraint [4], for the radial changes described in this Section.
- The azimuthal overlap of the NB layout was clearly over-estimated, at least for the middle and inner rings.

As a result, we have radially relocated (see below) detectors of the TDR design on the forward wheels, with the aim of providing a wheel design that meets the existing ID specifications of hermeticity. Then, using (largely) an optimization of the wheel positions that reduces the level of <3 point tracks to ~ 1 per mil, and geometrical constraints, we demonstrate a satisfactory forward wheel geometry (called the NEW-B geometry).

4.1 Wheel Design

The active radial dimensions of detectors fabricated according to the TDR design are shown in Table 7. In keeping with the program construction, and a decision of the SCT Steering Group related to the detector design, we assume a fixed angular strip pitch of respectively 0.2081 mrad for the inner/middle rings. We keep 0.1615 mrad for the outer rings as for the TDR, NB and NEW-A layouts. This means that detectors of the TDR design can be used and for the middle and inner rings are a conservative choice).

The radial position of each detector has been adjusted using

- an outer active radius of 56.0 cm radius (along the detector median plane),
- a bonding gap of 2.1 mm (c.f. 2.2 mm for the TDR)
- a radial relocation to prevent gaps between modules based on a 31 mm wheel thickness (as compared with 26 mm for the TDR).

The radial detector positions on each wheel are shown in Table 7, for each of the TDR and NEW-B designs. Also shown are the active detector pitches assumed. The radial positions of the inner and middle detectors have been motivated by the requirement of limited acceptance loss. The overlaps for each side of the outer (middle) wheels are 1.601 mrad (1.37 mrad), as compared with a requirement of 0.6198 mrad (0.806 mrad) for a 0.5% overlap on each detector side. Figures 4-1 a) and b) shows the distribution of the overlapping space points in wheels # 1 and #6, at z-positions of respectively 0.8385 m and 1.695 m. Table 8 shows the probability per track of that no space point is reconstructed in the wheel (gap), and the probability of an overlap in each of Φ and radius. Using the current design, Φ overlaps remain comfortable for both hermeticity and alignment, and the performance could profit from a longer middle and inner detectors at the expense of overlap. In both the NB and NEW-B wheel geometries, the R_{out} overlap (wheel

#1) and R_{in} overlap (wheel #6) are marginal but still acceptable (see the previous comment in this context).

We conclude that a wheel geometry using the existing TDR detector design is satisfactory, and as good as that of the NB layout.

.

	TDR				NEW-B		
Detector	r_{in} cm	r_{out} cm	Pitch r_{in} µm (mrad)	Pitch r_{out} µm (mrad)	r_{in} cm	r_{out} cm	Assumed pitch (mrad)
W11	25.919	33.11	54.4 (0.2099)	69.5 (0.2099)	26.139	33.33	0.2081
W21	33.4916	39.7625	70.3 (0.2099)	-	33.7116	39,9825	0.2081
W22	39.9825	45.18	-	94.8 (0.2098)	40.2025	45.39	0.2081
W31	43.8666	50.2245	70.8 (0.1614)	-	43.8766	50.2345	0.1615
W32	50.4445	56.0	-	90.3 (0.1613)	50.4445	56.0	0.1615

TABLE 7. Detector and wheel geometry of the TDR design, and as assumed for the NEW-B design. For the inner and middle rings, the NEW-B design assumes a smaller detector dimension that the TDR design (this could allow an extended radius if a re-design was made).

.

	Wheel #1	Wheel #6
Gaps	1.91×10^{-2}	1.75×10^{-2}
Overlaps in Φ	1.87×10^{-2}	1.93×10^{-2}
Overlaps in R(out)	0.42×10^{-2}	2.59×10^{-2}
Overlaps in R(in)	2.70×10^{-2}	0.39×10^{-2}

TABLE 8. Probability per track that no space point is reconstructed (gap), or that overlapping space points are reconstructed, for the NEW-B layout in the range $1.0 < |\eta| < 2.47$.

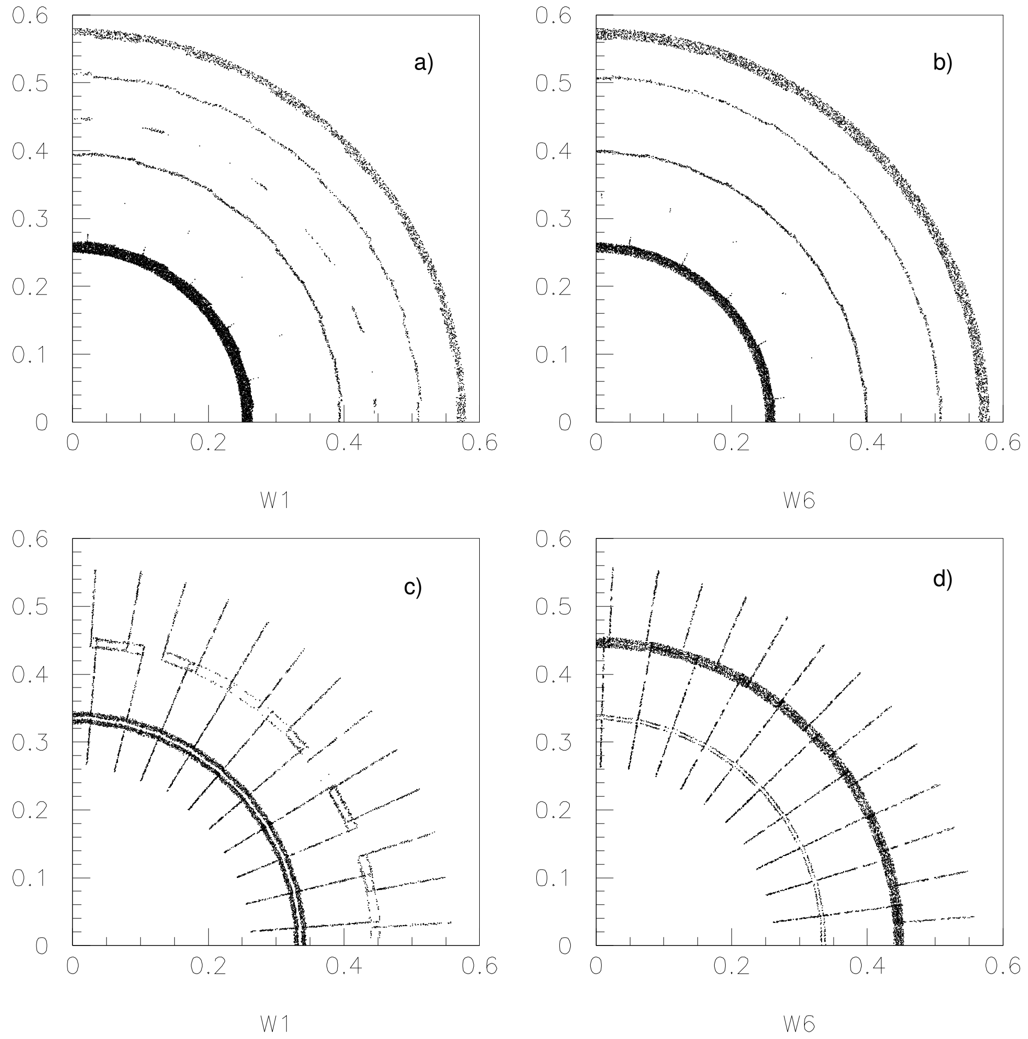

Figure 4-1 Tracks having no reconstructed space point in either wheels 1 (a) or 6 (b), for the NEW-B layout. Figures c) and d) show, for the same wheels, events for which there are overlaps between modules [3].This plot includes the event category for which there are 'Φ- overlap space points'

4.2 Wheel positions in the NEW-B layout.

On the basis of the wheel design described above, an optimization of the wheel positions has been made. Taking into account

- geometrical constraints (for example the position of the 1st wheel, and constraints defined by the design acceptance of $|\eta| < 2.47$),
- the need to equalise the spacing between the wheels where this is feasible, and
- the need to avoid projectively aligned bond gaps,

we have optimised the z-position of the wheels to ensure a 3-point track loss of less than 1 per mil).

The final wheel positions are listed in Table 9, where they are also compared with the NB and TDR layouts. The following points are possibly useful to note.

- The external active radius of 56.0 cm is a major constraint in the layout.
- The wheel # 2 position is a compromise between the acceptable rate of tracks having < 3 space points, and the requirement to optimize the wheel #1 - wheel # 2 separation. That rate has nothing to do with the additional ring of the NB design.
- The positions of wheels #7 to #9 are determined by the acceptance, with minor deviations due to existence of projectively aligned bond gaps. Wheel #3 has also been moved to smaller |z| with respect to the TDR and NEW-A layouts, to avoid aligned bond gaps.
- There is considerable flexibility in the choice of wheel #5 and wheel #6 positions, and an attempt has been made to equalise the wheel spacing.

.

Disk #	NEW-B Layout (metres)	NB Layout (metres)	TDR layout (metres)
1	0.8385	0.84	0.835
2	0.922	0.906	0.925
3	1.063	1.0575	1.0720
4	1.260	1.2775	1.260
5	1.470	1.5110	1.46
6	1.700	1.7450	1.695
7	2.070	2.0610	2.135
8	2.440	2.52	2.528
9	2.735	2.735	2.778

TABLE 9. Z-position of disks in the NEW-B, TDR and NB layouts

The NEW-B layout is shown in Figure 4-2, and the rate of tracks with respectively <4 or <3 reconstructed space points is shown in Table 10, and Figure 4-3 a). The design goal of a low rate (< 1 per mil) of reconstructed tracks having < 3 SCT space points is maintained. As shown in Figure 4-3 b), the radial separation of space points is improved for the NEW-B layout.

	NEW-B Layout	NB Layout
Fraction of tracks with <4 reconstructed SCT space points	0.061	0.056
Fraction of tracks with < 3 reconstructed SCT space points.	9.61×10^{-4}	3.72×10^{-4}

TABLE 10. Fraction of tracks with respectively < 4 and <3 reconstructed SCT space points, for the NEW-B and NB layouts, in the range $1.0 < |\eta| < 2.47$.

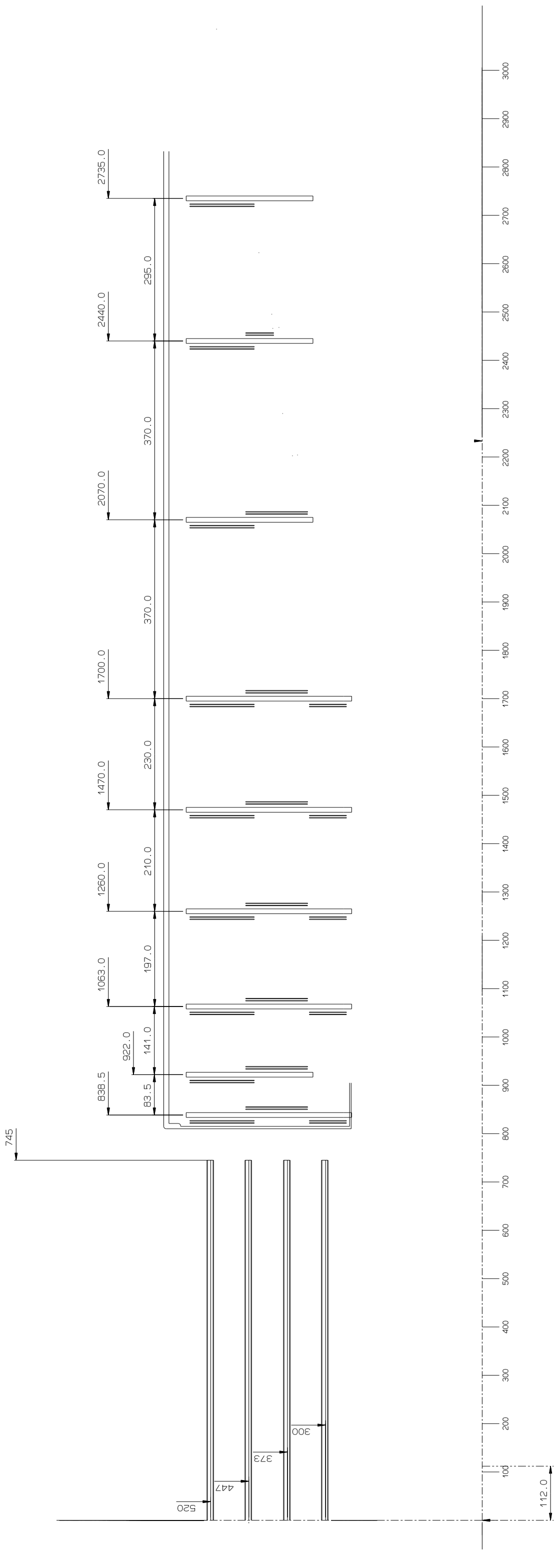

Figure 4-2 Layout NEW-B

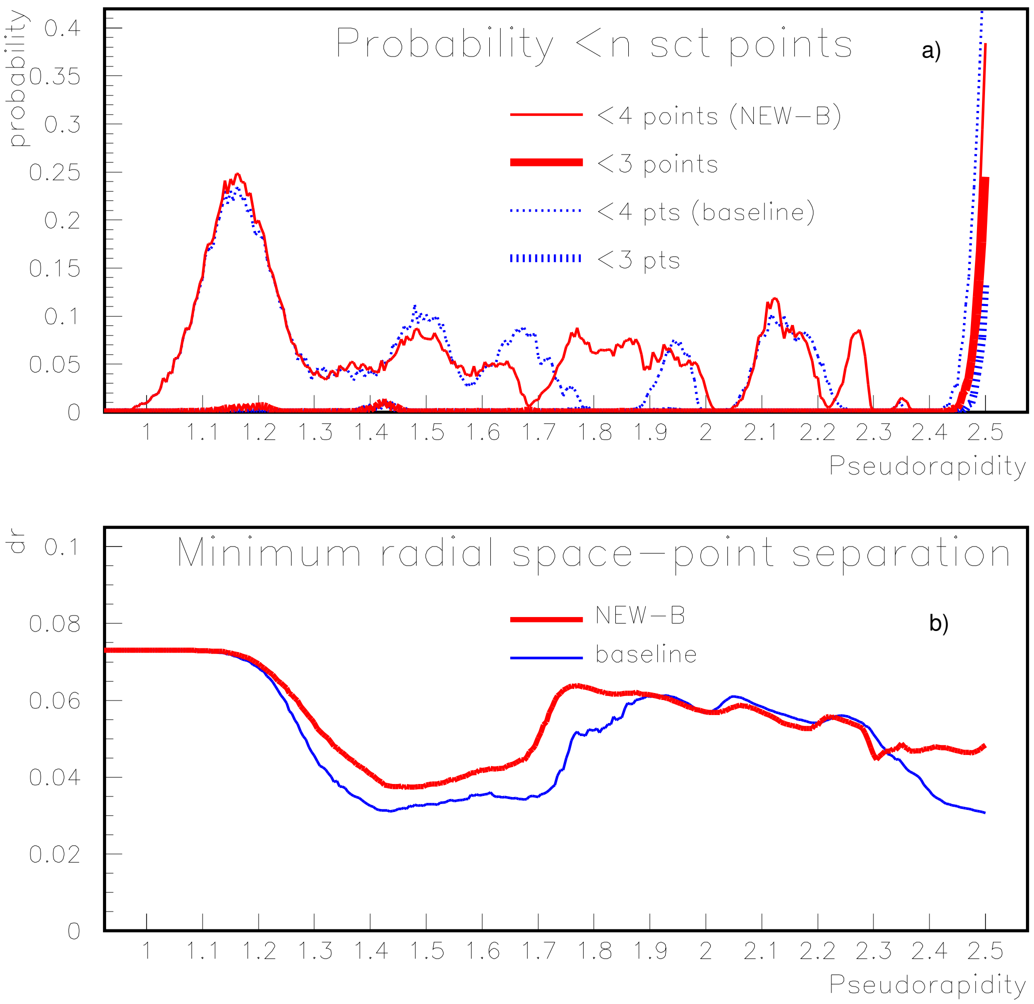

Figure 4-3 Fraction of tracks (a) as a function of $|\eta|$, for which respectively < 4 or <3 space points are reconstructed by the SCT. Both the NEW-B and NB layouts are shown. The figure (b) compares the minimum radial separation between reconstructed space points, for each layout.

5 The NEW-C and NEW-D Wheel Designs.

Following a presentation of the NEW-B layout, it was requested that a new disk optimization be performed for a disk thickness of 32 mm, and with an optimization of all detector shapes. Because of the marginal differences with respect to the NEW-B layout, we present 2 possible disk layouts:

a. Design NEW-C assumes an optimised detector disk for the outer, middle and inner modules of the disk.

b. Design NEW-D assumes the TDR detector shape for outer modules, and optimised detector shapes for the middle and inner rings.

In each optimization, the following constraints are assumed

c. An overlap in Φ is required which is the maximum of a 0.5% overlap at each edge (rounded up to integral strip width), and the overlap required for wheel 1 hermiticity for tracks of p_T = 1 GeV/c (outer radius of each module type)

d. A maximum active silicon wafer radius of 43.3 mm (this compares with ~43.7 mm for the barrel detectors)

e. An adequate radial overlap in the limiting cases of wheel 1 and wheel 6.

The resulting detector geometry is shown in Table 11 for the NEW-C design, and Table 12 for the NEW-D design..

	NEW-C Wheel Design						
Detector	r_{in} mm	r_{out} mm	Pitch r_{in} µm	Pitch r_{out} µm	Pitch (mrad)	$y(r_{in})$ mm	$y(r_{out})$ mm
W11	259.983	332.2	53.8	68.8	0.207	20.763	26.531
W21	335.805	399.107	69.5	82.6	0.207	26.819	31.874
W22	401.207	454.0	83.0	94.0	0.207	32.042	36.258
W31	437.469	501.627	70.0	-80.37	0.160	26.982	30.939
W32	503.727	560.0	80.6	89.6	0.160	31.069	34.540

TABLE 11. Detector and wheel geometry of the NEW-C design.

	NEW-D Wheel Design (TDR detector shapes for W31, W32)						
Detector	r_{in} mm	r_{out} mm	Pitch r_{in} µm	Pitch r_{out} µm	Pitch (mrad)	$y(r_{in})$ mm	$y(r_{out})$ mm
W11	262.038	334.05	54.2	69.1	0.207	20.927	26.679
W21	337.658	400.703	69.9	82.9	0.207	26.967	32.002
W22	402.803	455.295	83.4	94.2	0.207	32.169	36.362
W31	438.766	502.345		-	0.1615		
W32	504.445	560.0	-		0.1615		

TABLE 12. Detector and wheel geometry of the NEW-D design.

Table 13 shows the overlap and gap contribution in the extreme cases of wheel 1 and wheel 6, for each of the NEW-C and NEW-B designs, and in comparison to the NEW-B design. There is little difference in the results (please recall the 31 mm maximum disk spacing of the NEW-B design, however).

.

	NEW - B		**NEW - C**		**NEW - D**	
	Wheel #1 (x 10^{-2} **)**	**Wheel #6 (x** 10^{-2}**)**	**Wheel #1 (x** 10^{-2}**)**	**Wheel #6 (x** 10^{-2}**)**	**Wheel #1 (x** 10^{-2}**)**	**Wheel #6 (x** 10^{-2}**)**
Gaps	1.91	1.75	1.86	1.77	1.84	1.76
Overlaps in Φ	1.87	1.93	1.22	1.28	1.23	1.29
Overlaps in R(out)	0.42	2.59	0.63	2.88	0.60	2.95
Overlaps in R(in)	2.70	0.39	2.94	0.60	2.96	0.53

TABLE 13. Probability per track that no space point is reconstructed (gap), or that overlapping space points are reconstructed, for the NEW-B, NEW-C AND NEW-D layouts in the range $1.0 < |\eta| < 2.47$.

Using the same wheel positions as described in Section 4 for the NEW-B design, the fractional loss of 4-point and 3-point hits in the NEW-C and NEW-D designs is shown in Table 14.

	NEW-B Layout	**NEW-C Layout**	**NEW-D Layout**
Fraction of tracks with <4 reconstructed SCT space points	0.061	0.059	0.061
Fraction of tracks with < 3 reconstructed SCT space points.	9.61×10^{-4}	7.62×10^{-4}	10.2×10^{-4}

TABLE 14. Fraction of tracks with respectively < 4 and <3 reconstructed SCT space points, for the NEW-B and NB layouts, in the range $1.0 < |\eta| < 2.47$.

It can be concluded that each of the NEW-B, NEW-C and NEW-D designs fulfil the tracker specifications, and that differences between the wheel layouts have a small effect as compared with extraneous effects such as detector inefficiency. For completeness the distribution of gaps on respectively wheel1 and wheel6, and the distribution of track losses as a function of |h| is shown in Figures 5.1 and 5.2 for the NEW-C layout.

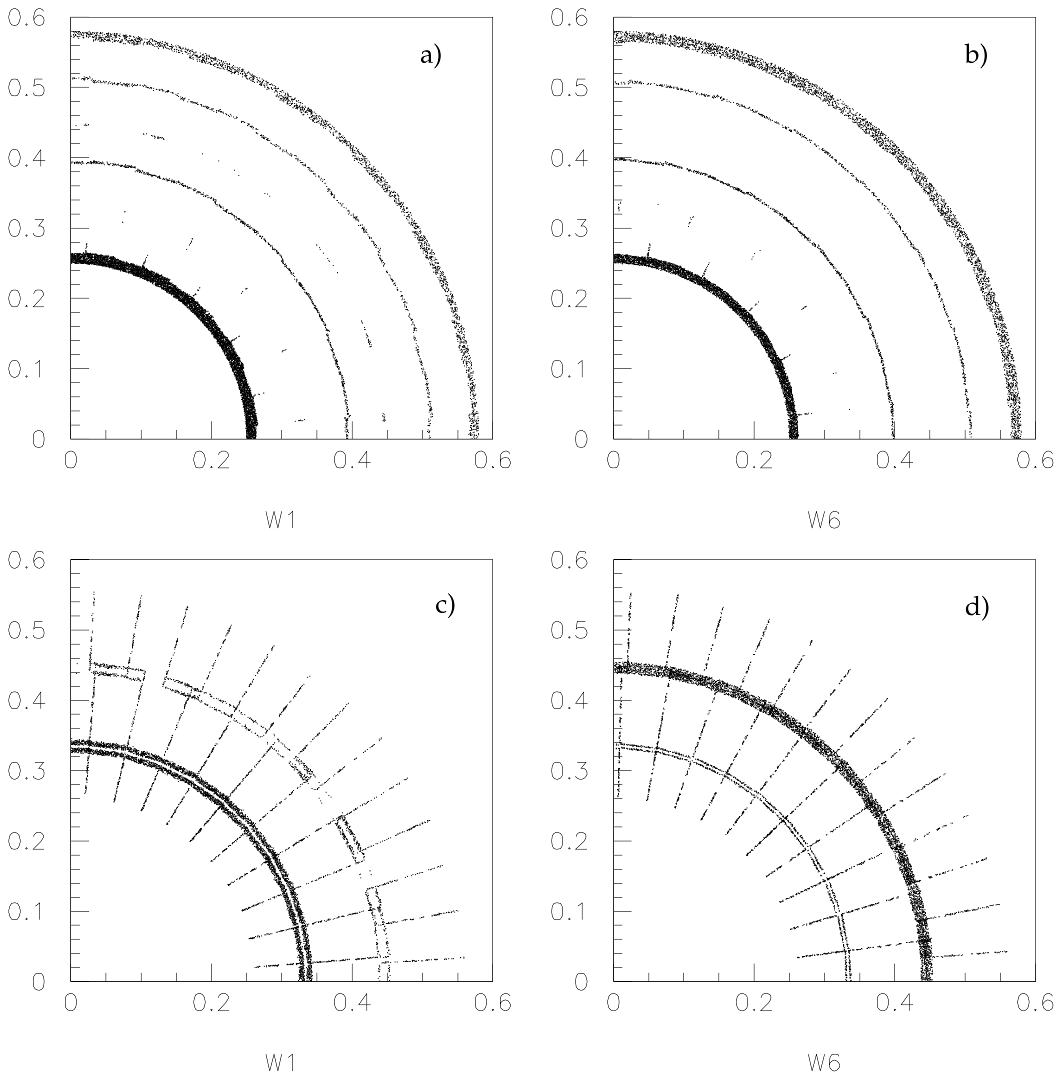

Figure 5-1 Tracks having no reconstructed space point in either wheels 1 (a) or 6 (b), for the NEW-C layout. Figures c) and d) show, for the same wheels, events for which there are overlaps between modules [3].This plot includes the event category for which there are ‘Φ- overlap space points’

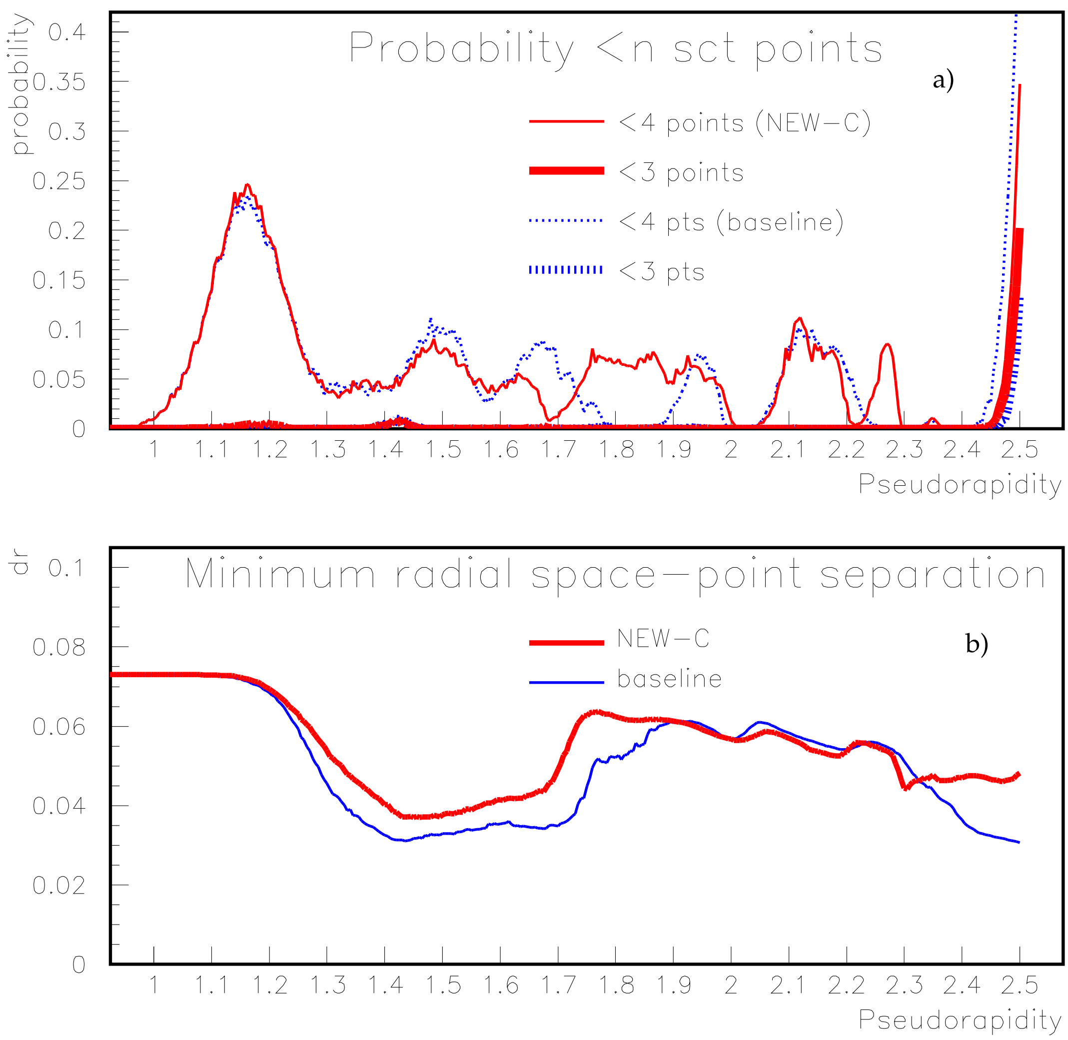

Figure 5-2 Fraction of tracks (a) as a function of |η|, for which respectively < 4 or <3 space points are reconstructed by the SCT. Both the NEW-C and NB layouts are shown. The figure (b) compares the minimum radial separation between reconstructed space points, for each layout.

6 Conclusions

We make the following conclusions.

1. Detector bond gaps result in a loss of hermeticity which is significant, and a forward layout optimization based only on hermeticity arguments (ignoring the bond gaps) is inappropriate.

2. A minimal change to the New Baseline layout (the NEW-A layout) retains reasonable hermeticity, improves the pattern recognition capability and avoids an inner module ring on wheel #2 (with consequent cost and material benefits).
3. Using the original TDR detector designs, with a slightly modified wheel layout, the performance specifications of the SCT Forward Tracker can be maintained using the NEW-B layout described in the text
4. The performance of the NEW-B layout could be further improved by a new optimization of the middle and inner detector dimensions. This has been done in the NEW-C and NEW-D layouts, with small improvements.

References

1 ATLAS Inner Detector TDR, Atlas Collaboration CERN/LHCC/97-16

2 New Baseline Layout. See WWW address of University of Liverpool, under heading of 'Layout' (http://hep.ph.liv.ac.uk:80/www/atlas/)

3 Private communication, E. Perrin. It is largely accepted that the disk thickness can be reduced below 34 mm. H. Becker [5] and the Nikhef group have suggested ways to retain a disk thickness of < 30 mm. The value of 31 mm was chosen for this exercise as a conservative limit assuming the existing cooling block design, 4 mm cooling tubes, and a 1 mm bond clearance.

4 Private communication, G. Tappern. E--mail of January 8th, 1999.

5 H. Becker, transparencies of the Cartigny Meeting on Forward Modules, November 1998.